Available online at www.easdprocedia.org
EASD Procedia EURODYN (2020) 2407-2426

EASD Procedia

EURODYN 2020
XI International Conference on Structural Dynamics
M. Papadrakakis, M. Fragiadakis, C. Papadimitriou (eds.)
Athens, Greece, 23–26 November 2020

REDUCING IMPACT OF VIBRATIONS FROM COMPACTION ON SLOPE STABILITY

Jörgen A.T. Johansson[1], Joonsang Park[1], Christian Madshus[1], and Carl Wersäll[2]

[1] Norwegian Geotechnical Institute
Sognsveien 72, NO-0866 Oslo, Norway
e-mail: jjo@ngi.no, jp@ngi.no, cm@ngi.no

[2] KTH Royal Institute of Technology
SE-100 44 Stockholm, Sweden
carl.wersall@byv.kth.se

Keywords: Compaction, slope stability, non-linear soil, and equivalent linear frequency domain FE

Abstract. *A tsunami caused by a landslide caused extensive damage at Statland, Norway in 2014. The landslide was probably triggered by man-made vibrations. To understand better how vibrations from vibratory compaction affect slope stability, a frequency domain numerical tool (Comsol Multiphysics) has been extended to account for realistic non-linear soil behaviour. The tool is validated by comparison with field experiments of vibratory compaction. The non-linear analysis is believed to capture the essential behaviour of the vibratory compaction and the response of the slope. The numerical analysis and evaluations indicate vibratory compaction can have contributed to triggering the slide at Statland. To perform compaction in the vicinity of slopes with low stability near the shoreline with vibration susceptible soils we suggest: 1) using lighter equipment and/or higher loading frequencies or performing compaction without vibration, and avoiding excessive jumping of the vibratory roller drum; 2) applying thinner layers and more time between compaction passes, allowing for drainage of potential built up pore pressures; 3) monitoring slope horizontal and vertical displacements at some critical points; and 4) monitor pore pressures at critical points, if possible.*

ISSN:2311-9020
Peer-review under responsibility of the Organizing Committee of EURODYN 2020.
doi: 10.47964/1120.9195.20234

1 INTRODUCTION

A landslide-induced tsunami caused extensive damage at Statland, Norway in 2014. Only luck prevented any fatalities. The investigation of technical cause [1] concluded the slide was likely triggered by vibratory compaction of a rockfill in the shoreline in connection with development and extension of a near shore recreation cottage area. For safer nearshore developments it is very important to understand better the processes involved in the landslide triggering.

Often ground conditions along the Norwegian fjords consist of loose soil deposits with silt and sensitive clays. In combination with artesian water pressure the stability of such shoreline submarine slopes can be very low. The combination of loose soil and low stability makes these slope extra vulnerable to vibrations.

A tentative procedure on how to account for cyclic- and dynamic effects during vibratory compaction near slopes with vibration sensitive material, was proposed [2]. However, such approach may not always be practical, especially in small projects. Therefore the possibility of establishing a vibration limit has also been investigated in [3]-[4]. Through linear elastic models accounting for soil non-linearity by an ad-hoc reduction of soil stiffness depending on the induced strains. Recently, an equivalent linear numerical tool has been developed which has been validated against data from compaction and pile driving vibration experiments [5]. This tool is applied to the Statland case to better understand how non-linear soil properties affect the dynamic response of the slope. The following section gives a brief description of vibration triggered landslides and soil compaction induced vibrations before describing the numerical model and results for the Statland case.

2 VIBRATION-TRIGGERED LANDSLIDES

It is commonly not considered likely for non-blasting construction vibrations to cause landslides. We have only found the following potential cases in the literature:

- The Trestyckevatten slide south of Uddevalla, Sweden in 1990 [6] was most likely triggered by a heavy vibratory roller which caused the failure of a berm designed to provide additional stability to an embankment for the E6 highway.
- The Åsele-slide in 1983, also in Sweden [7] caused the failure of a road embankment that was partially submerged due to filling up of hydro-electric reservoir. The slide was triggered by tractor- pulled 3.3 ton vibratory roller.
- The 1987 Lake Ackerman slide caused damage to Highway 94 in Michigan, USA [8]. Six 22-ton trucks with vibrator plates generating signals for a seismic refraction study triggered the slide. The road embankment consisted of hydraulic fill of loosely deposited sand. Hryciw et al. estimated the cyclic shear strains induced in the fill of up to 0.06%, which could be enough to generate pore pressure build up and cause failure in loose fine silty sand ([9], [10]).
- The 1994 Skagway landslide reported in [10] have similarities with the Statland case, however there is limited information on the road construction done shortly before the slide. It is not clear if compaction can have contributed to the landslide.

The above cases were all near shoreline submarine landslides with loose ground conditions. For landslides where rock blasting was a potential trigger, the slide occurred in combination with other adverse factor such as low stability prior to blasting, higher than normal ground water level due to high precipitation, artesian pressures, erosion at the slope base, temporary placement of fill masses, etc. In addition, the existence of thin sand or silt layers within the clay are

confirmed in many cases, and are hence assumed to have played a crucial role [12]-[13]. These adverse factors also play an important role, when construction vibrations induce landslides.

3 STATLAND LANDSLIDE

January 29, 2014, a submarine landslide and a resulting tsunami [14] caused damage to port facilities and nearshore infrastructure at Statland, in the county of Nord-Trøndelag, Norway. Some photos of the damage are shown Figure 1. The newly constructed road and part of an old molo was swept away by the landslide. Luckily no humans was in vicinity when the landslide occurred. The tsunami slammed into buildings many of which were totally or partially destroyed. The investigation of the possible slide causes [1] established the slide occurred an hour and half after the filling and compaction work was finished. It further concluded it was very likely the construction work triggered the slide.

Deltaic deposits have accumulated over years along the margin of Namsfjorden outside the small community of Statland. The deposits consist mainly of loose sands and silts overlaying marine and partly sensitive clays (quick clays). The soft and weak soil conditions result in very low static factors of safety for the partially submarine slope [1]. In addition, there are considerable amount of organic material down to depths of 14 m beneath the seabed [1], which originated from sawmill industry in the area during the last 120 years. The sedimentation rate in the area is estimated to be in the order of 12 cm/year. Thus, there are considerable amounts of material still undergoing consolidation.

Such loose silty soils are susceptible to strength degradation due to vibrations, and thus some preliminary analysis of the impact of vibratory compaction on the slope stability was performed in [1]. The analysis indicated that compaction may have contributed to slide triggering in combination with other factors such as low tide and low static stability.

Figure 1 Photos showing damage caused by the Statland landslide. The right hand side photos compare the situation before and after the landslide with yellow dashed line showing the shoreline after the slide.

4 VIBRATIONS FROM VIBRATORY ROLLERS

Ground vibration from vibratory rollers transmits large dynamic loads to the soil in order to compact the fill materials during construction. Such dynamic loads can possibly cause pore pressure build-up and reduce soil strength in vibration susceptible soils such as loose silt and sand, and sensitive clays. This should be considered when carrying out construction work near slopes with such soils. The strength reduction depends on soil conditions, cyclic load amplitude and number of load cycles.

Performing vibratory roller compaction according to guidelines such as the Norwegian standard NS 3458 involves passing over the same area sometimes up to 8 times with the roller. This means a soil element is exposed to a large number of vibration cycles. The number of cycles depends on the speed of the roller and the vibration frequency. Vibratory rollers have vibration frequencies typically between 20-40 Hz and, on some rollers, both the load amplitude and vibration frequency can be varied, depending on the type of soil and the thickness of the compacted layers. The speed of the roller is typically between 0.5 m/s to 1.5 m/s. E.g. for the case of the Statland landslide ([1]) a low estimate of number of cycles indicated the soil in the upper part of the slope had experienced several hundred cycles with strains large enough to build up pore pressure.

The vibration amplitude depends on the vibratory roller's dynamic behaviour and its interaction with the ground during the compaction process (see e.g.[14]and [16]). There are various vibration modes, changing from full contact between drum and the substrate, to the periodic loss of contact during normal operation, to a less desirable chaotic bouncing of the drum as shown in Figure 2. Bouncing occurs when the period for one cycle is longer than the time for loss of contact and is more common at larger load amplitudes and can cause increased vibration amplitudes.

Vibratory compactors can start bouncing when the compacted fill is becoming stiffer after a number of passes over the fill. When this happens the roller drum will lose contact with the soil during a longer part of each vibration cycle and therefor do not vibrate with the same frequency as the compacted fill and soil. When bouncing occurs the soil is subjected to load impulses with a frequency which can be closer to the soil deposit's natural vertical vibration frequency. This can lead to larger vibrations and possibly pore pressure build up further away from the roller. There may be a "double" resonance if the natural frequency of the vibratory roller and the underlying fill is close to the natural vibration frequency of the soil layers in the slope.

Full-scale tests of vibratory compaction [17], [18] indicate the largest vibration amplitude occurs when the drum vibration frequency is about twice of the natural vertical vibration frequency of the system consisting of the drum and underlying fill and soil as shown in Figure 6. This is interpreted as that every other cycle the roller is in the air, and every other cycle it "hits" the compacted fill and soil in phase with the natural vibration frequency between roller and fill.

Jumping reduces the compaction efficiency [17] and is undesired. Therefore, some modern vibratory roller have various types of automatic feedback control systems to avoid such jumping [12]. The jumping is reduced by changing drum vibration amplitude and/or frequency ([19]). Since jumping can cause larger vibrations it is also undesired with respect to slope stability and should be avoided. The lower graph in Figure 2 shows schematically the dynamic behaviour of a vibratory roller drum and the vibration frequency halving which can occur during jumping.

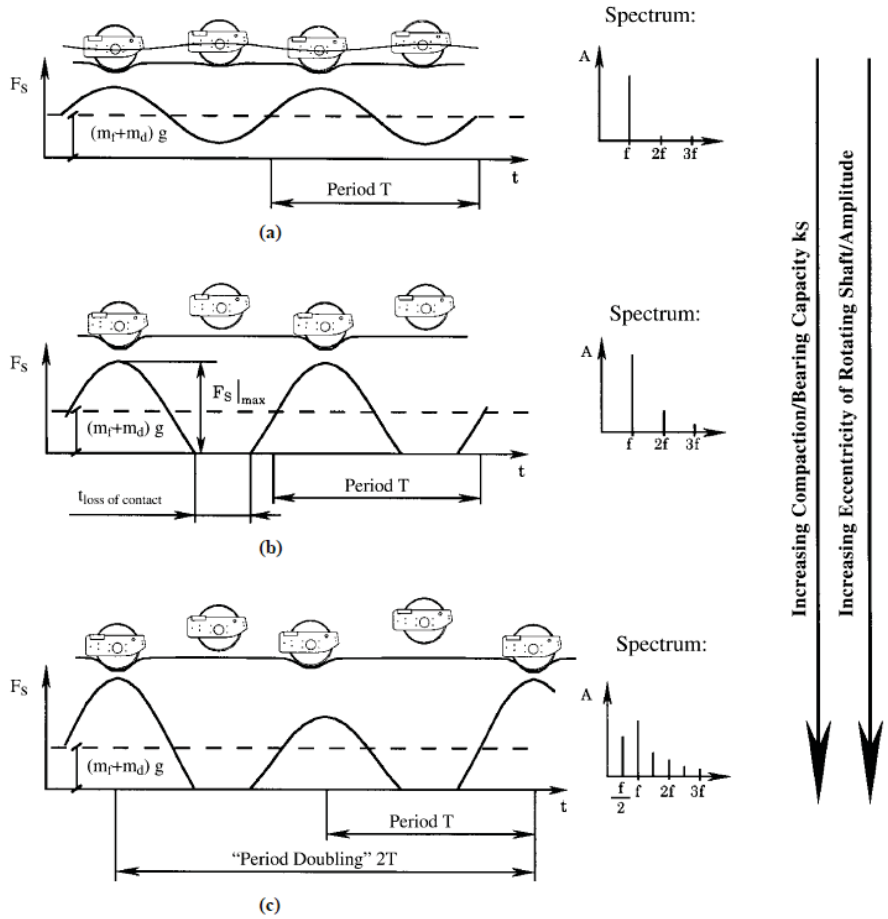

Figure 2 Dynamic behaviour of a vibratory roller drum, a) full contact, b) periodic loss of contact, and c) double-jumping. Spectrum show the period doubling when the drum jumps. From [19].

5 NUMERICAL METHOD

Numerical simulations of effects from vibro-compaction done earlier in [2]-[4] were based on linear elastic material properties. Soil nonlinearity (reduction of stiffness with increased loading) was accounted for by manually reducing the material stiffness in the regions subjected to the largest cyclic strains. Recently we implemented a new feature in Comsol Multiphysics [5], to account directly for soil nonlinearity by means of laboratory measured strain dependent secant stiffness and damping. This extended tool is described in the following sections. The analysis is done in the frequency domain which allows for an equivalent linear soil model to be used to iteratively account for soil non-linearity.

Modelling of nonlinear soil behaviour with the equivalent linear method originates from the analysis of earthquake induced ground vibrations [21][22]. With increasing cyclic strain, the secant soil stiffness decreases, and the damping increases as shown schematically in Figure 3. This behaviour is often represented by curves showing reduction of secant shear modulus and increase of damping as shown in Figure 4.

The input parameters in the model is the initial shear wave speed, mass density, and hysteretic damping. In the frequency domain analysis constant elastic parameters are used, and thus the nonlinear stress-strain variation cannot be followed. Therefore, for each loading frequency, the COMSOL solver iterates until there is shear modulus is compatible with the shear strain in an equivalent linear sense in the whole computational domain. The secant shear modulus and damping vary with the distribution of shear strain amplitude within the soil around the roller

drum. The secant shear modulus, G_s, is expressed as varying with the octahedral shear strain amplitude, γ, according to the hyperbolic relationship in Eq. (1).

$$G_s = G\frac{1}{1+\left(\frac{|\gamma|}{\gamma_{ref}}\right)^n} \tag{1}$$

where G is the initial shear modulus, n and γ_{ref} are material parameters. The octahedral shear strain, γ, is a complex variable when operating in the frequency domain, and therefore the equation was modified in COMSOL to use the amplitude of the shear strain. The material damping is modelled with a frequency independent damping, which is included in the soil stiffness by replacing the shear modulus with a complex shear modulus, $G_s^* = G_s(1+i2D)$, where, D is the material damping factor, and i the imaginary unit.

The above method is not restricted to the hyperbolic law in Eq. (1), other formulations such as presented in [23]-[26], or simple tabulated data points for shear strain versus G/G_s , or damping, for specific materials are also possible. The material damping for the current analysis were given as tabulated values.

The combination of a cyclic and an average shear stress, can have considerable effect on the cyclic stress-strain behaviour and damping [27]-[29], but these effects were not considered in this study. Though the nonlinear cyclic stress-strain and damping-strain behaviour of the clay, silt and sand materials differ to some extent, in this preliminary study, they were modelled with the same stiffness reduction and damping curves, based on the empirical equations in [23] with the soil index input parameters given in Table 1.

Parameter	Value	Unit
Plasticity Index, PI	20	%
OCR	10	1
σ_o'	100	kPa.
n	0.98	1
γ_{ref}	0.075	[%]

Table 1: Input parameters for modulus reduction and damping curves.

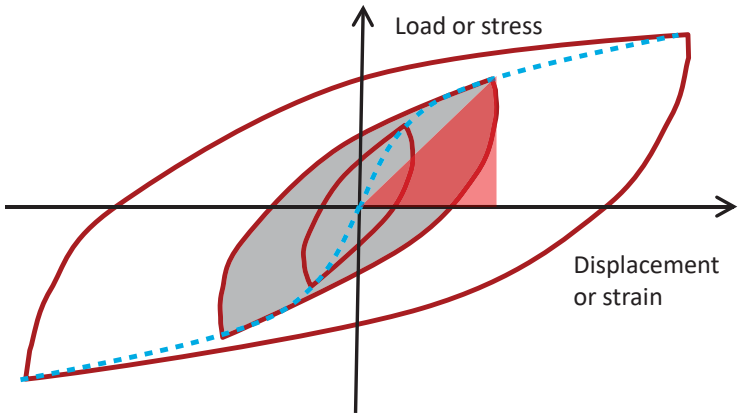

Figure 3 Schematic cyclic stress-strain loops for a soil element. The red triangle and the grey shaded loop shows the definition of elastic energy and hysteretic loss energy respectively in one cycle. The cyclic "back-bone" or "skeleton" curve which controls the shape of the hysteresis loops, is shown by the blue dotted line. Assuming a hyperbolic shape this line is given by Eq. (6).

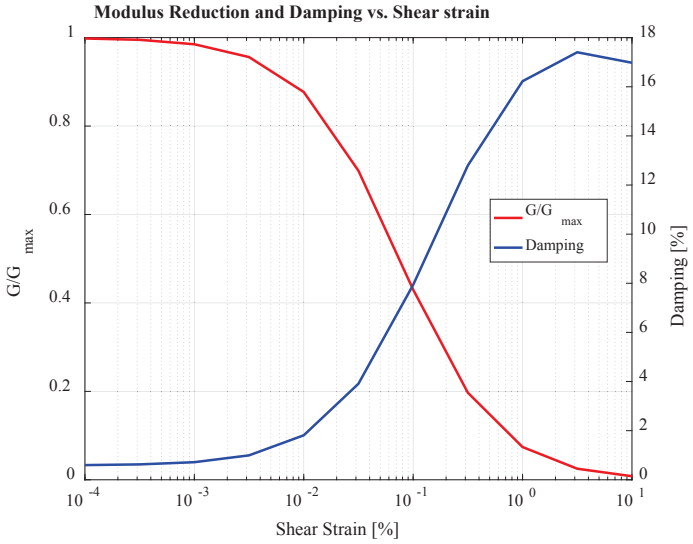

Figure 4 Shear Modulus reduction and damping versus shear strain used in COMSOL analysis.

Absorbing boundaries of the Perfectly Matched Layers (PML) type [30] are used to reduce unwanted wave reflections from the boundaries of the computation domain in the dynamic analysis. This also allows for modelling of radiation damping.

Since the soil strains become large near the vibratory roller it is important to have mesh element size fine enough to resolve the high strain and stress gradients. A comparison between *1st* and 2nd order elements are given in section 7.2. Also the element size should be small enough to resolve the wave lengths appearing for the various stress and strain conditions at the various frequencies analysed. In three dimensions it is most likely faster to adopt the mesh size according to the frequency, i.e. the higher frequency the finer the mesh. In 2D we have found for some models it was faster to use "brute force" and use the same fine mesh for all frequencies.

6 VALIDATION BY COMPARISON WITH FULL SCALE VIBRATORY ROLLER COMPACTION EXPERIMENTS

A qualitative comparison of the vibratory roller drum vertical displacement amplitude is shown in Figure 5. The left figure show measured response in the field [19] and the right figure show simulated response for 3D model as described in section 7, for several load amplitudes constant with frequency. The maximum applied load amplitude is 258 kN shown with light blue line with circle – marked 1 in the legend, the other curves are for lower load amplitudes as indicated by the numbers in the legend. The figure clearly demonstrates that the developed model is able to capture the resonance frequency reduction with increasing load amplitude as it appears due to resonance match with the roller vibration frequency. Some data points are missing in the computation due to lack of convergence in the solver which tends to appear at very large vibration amplitudes. Improved convergence can likely be achieved with a finer mesh.

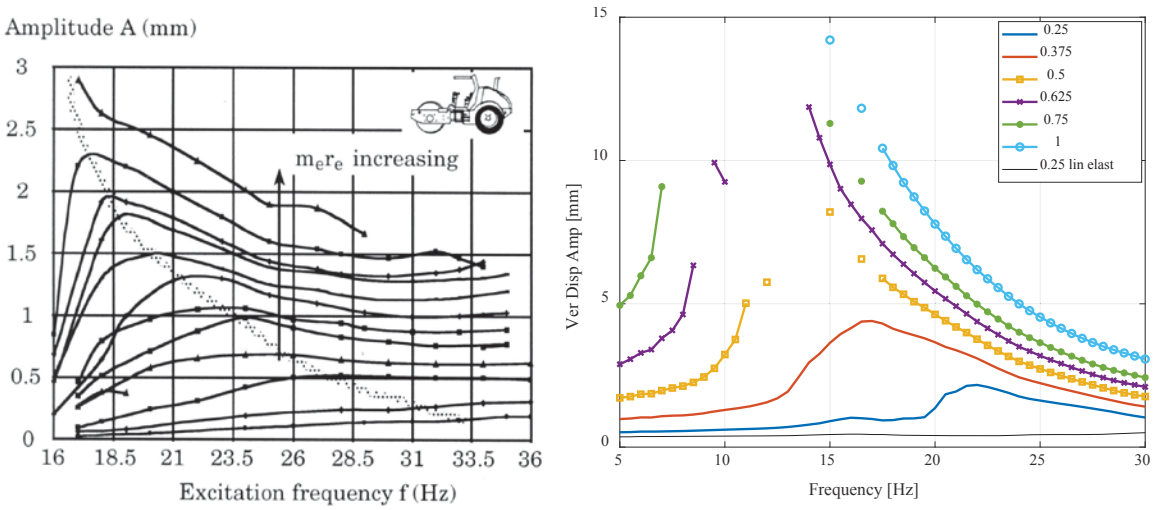

Figure 5 Qualitative comparison vibratory roller drum response to capture the change of resonance frequency due to increasing load amplitude. The left figure is from [19].

To demonstrate quantitatively the equivalent linear method can capture essential features of nonlinear dynamic soil behavior during vibratory compaction, we have compared numerical results with full-scale compaction experiments described in detail in [17] and [18], and in references therein. Several frequency sweep tests were run with the roller passing over an area being compacted. The vertical displacement amplitude of the roller during the sweep tests are shown in Figure 6 a). Within each pass over the compacted area, the frequency is "swept" from 15 to 35 Hz. With increasing number of passes of the vibratory roller, the frequency of the first peak found between 15 and 20 Hz increases due to increasing soil stiffness due to the effect of the compaction. The second peak in each curve at about 30 Hz is due to the drum is bouncing.

An axi-symmetric model was used for quick analysis of the vibro-compaction experiment. The drum, the compacted gravel layer and the underlying rock fill were modelled with 2nd order solid finite elements. Absorbing boundaries was applied on the outer and bottom boundary of the model. A stiff block with a mass of 7600 kg represents the roller drum. The vertical dynamic load on the drum, due to an eccentric moment of 7.3 kgm, is proportional to the square of the rotation frequency giving a load amplitude of 83 kN at 17 Hz increasing to 258 kN at 30 Hz. The depth to bedrock was assumed 5 m in the model.

To account for the densification during compaction, the model was run with different initial shear wave speeds in the gravel fill layer of 160, 180, 200 and 220 m/s. A Poisson's ratio of 0.3 was used in the gravel fill. The rock fill shear wave speed was assumed to vary linearly between from 220 m/s beneath the fill to 270 m/s at 5 m depth. The rock fill density and Poisson's ratio were set to 2000 kg/m^3 and 0.3 respectively.

To model the effect of soil nonlinearity on the response of the drum, the curves for shear modulus reduction and damping versus shear strain shown in Figure 3 were used for the gravel fill. For simplicity, the same curves were used for the rock fill as well.

Varying the initial shear wave speed from 180 m/s to 220 m/s gave a good match with the frequency variation of the first frequency peak observed in the experiment as can be seen in Figure 6 b). The 2nd response peak is due to bouncing of the drum and is not possible to account for in the numerical model due to assumption of full contact between drum and soil.

The experimental response amplitude at the higher frequency of 30 Hz, is not very much higher (~20%) than the response at 15 Hz. Thus the load amplitude experienced by the soil in the experiment when the drum vibrates with 30 Hz and bounces is likely not much larger than the one at 15 Hz.

The analysis show it is necessary to use a nonlinear soil behaviour to obtain a good match with the frequencies observed in the experiments. As shown in Figure 7 the computed shear modulus reduces to less than 10% of its initial value beneath the drum and the material damping factor exceeds 15%. There are many uncertainties in the non-linear modelling in terms of physical input parameters and the numerical model itself. However, the good match with experiments give confidence the method could be used for the analysis of vibro compaction near slopes and other related applications where the nonlinear soil behaviour is important, e.g. foundations subjected to large dynamic loads [5].

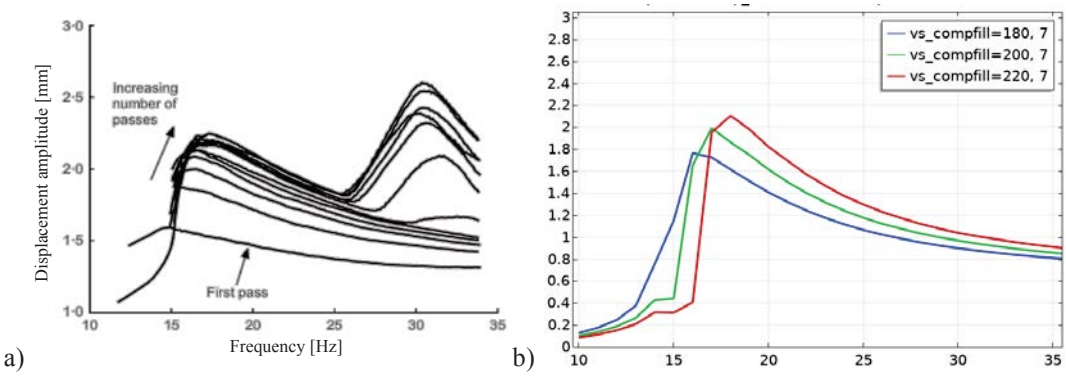

Figure 6 Vertical displacement amplitude of vibratory roller drum in frequency sweep test. a) Experimental result (Modified after [17]). b) Numerical results.

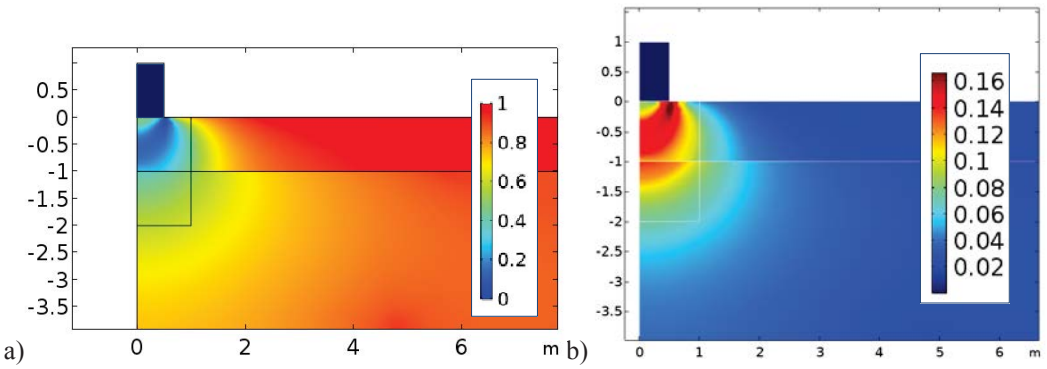

Figure 7 a) Shear modulus reduction and b) soil damping factor beneath vibrating block representing roller drum at 17 Hz for an initial shear wave velocity of 200 m/s in the fill layer.

7 VIBRATION ANALYSIS OF THE STATLAND LANDSLIDE

7.1 Numerical model

A three-dimensional calculation model was established (shown in Figure 8) based on the 2D geometry used in the investigation of the cause of the slide [1]. The colours indicate the shear wave speed as determined from CPT tests made at the site, with interpretation based on empirical equations from [31]. A road was constructed by compacting a rock fill layer (upper most yellow layer) and replacing older loose fills (in turquoise). Older fill material which was not replaced is shown in light green. The old fill contains various materials such as wood chunks etc. The shear wave speed in the replaced masses and in old fills are based on NGI's experience with similar materials [1]. The bed rock is modelled linear elastic with an assumed shear wave speed of 2000 m/s (shown in blue). Above the bedrock there is loose recently deposited material consisting of sand, silt and quick clay with shear wave speeds decreasing with depth from over

200 m/s between of 2 m to 3 m depth beneath the sea floor to about 100 m/s at 25 m depth. This was modelled with three thicker layers in yellow, orange, and red with constant initial shear wave speeds of 150, 120 and 100 m/s respectively. The Poisson's value in the fill mass is set to 0.4 and in soil below ground water level 0.495. The water above the submerged part of the slope has not been modelled. For an analysed vibrating submerged foundation under similar conditions, the water was shown to increase both radiation damping and added soil mass [32][33], thus it will likely have an effect of the dynamic response of the slope, but it is neglected here.

There was no information available about stress-strain curves for the materials at the time of analysis, therefore for simplicity, in the current model the same relative shear modulus reduction versus strain curve was applied to both fill and natural soil. The natural soil is very loose and as such the modulus-reduction curve may give a too stiff response. However, the objective was to estimate the order of magnitude of the induced strains in the soil.

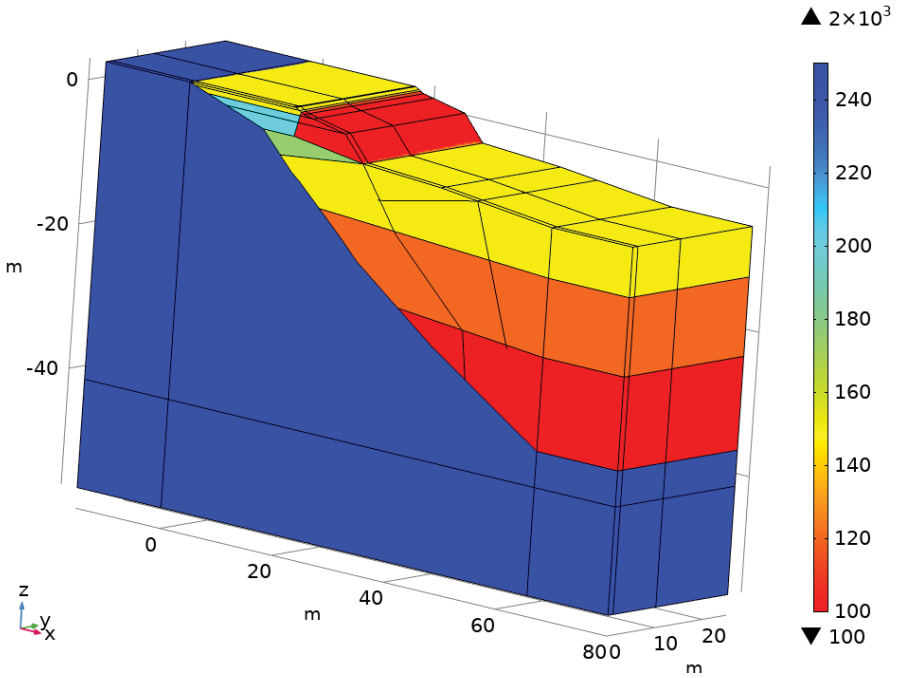

Figure 8 Model used for the vibration analysis of the Statland landslide case. Colours show shear wave speed in the fill and natural soils. The bedrock shear wave speed was set to 2000 m/s (shown in blue).

The vibratory roller used during the compaction work was a Volvo CE SD 115D with a 2.1 m wide and 1.5 m diameter drum. Further technical information about the vibro compactor is available in [34]. The part of the drum in contact with the soil is modelled as a 2.1 m long, 0.3 wide and 5cm thick, rigid plate placed close to the edge of the slope (as shown in Figure 10). The plate mass is equal to the dynamic mass of the whole drum, which was estimated to 3570 kg based on the nominal displacement amplitude of 1.92 mm and load amplitude of 257 kN at a vibration frequency of 30.8 Hz. The Young's modulus of the plate was set to a high value to simulate the drum to be very rigid. The load due to eccentric mass was applied uniformly on the plate and there is no slippage allowed between the plate and the soil. Most vibratory rollers can only operate within a few pre-set frequency values. Here we assumed the load is continuous in the range from 0-30 Hz and proportional to the square of the drum vibration frequency, similar to the load in the full-scale experiments [17].

The static stresses from the weight of the vibratory roller may somewhat increase the stiffness and strength of the soil beneath the drum, but this is not accounted for in analysis. The static load diminishes quickly with depth as opposed to the dynamic loads which penetrate

much deeper. As a verification, the static stresses in the model due to the weight of the plate have been compared with field measurement [35] of a similar vibro compactor. The stresses are of the similar magnitude. Analysis performed in connection with the validation showed the increase in static stress beneath the drum has little effect on the overall vibration response. It was checked by changing low strain shear wave speed with 25% in the layer closest to the drum resulting in 10% change in resonance frequency. This was considered to have little consequence for computing the dynamic effects of vibro compaction on slope stability.

7.2 Effect of soil non-linearity and frequency dependent load

The numerical 3D model is still under development with tuning of mesh size and discretization to handle the large strains in the vicinity of the drum. However, the numerical results are considered to still be informative for engineering purposes and are therefore presented here.

Figure 10 shows the vertical response of the drum with blue curves for a load increasing with the square of the vibration frequency from 10 kN at 5 Hz to 257 kN at 31 Hz. The peak response, taken as average of the two points on the plate, is 3.5 mm at 20 Hz for a load of 109 kN. The drum response increases rapidly when the load frequency approaches 20 Hz due to local resonance between the drum and soil immediately beneath it.

At 4 m below the drum and 10 m further out in the slope (locations indicated with arrows in Figure 10) the vibration amplitude (shown with green and red curve in Figure 9) increases when approaching 15 Hz, which appears to be the natural frequency of the slope. The vibration further away from the drum do not increase above 15 Hz even though the load amplitude and the drum response increases very much at that frequency. This is interpreted due to 1) the soil can only transmit a limited shear stress due to the non-linear soil behavior [31] and 2) the increasing dynamic resistance due inertia of the vibrating plate. This is also indicated by the maximum shear strain plots for 14 Hz and 20 Hz (Figure 10 and Figure 11). For vibration frequencies below 15 Hz there is very low shear strains except in the vicinity of the drum. For vibration frequencies of 20 Hz and above, the shear strain amplitude do not increase very much even though the load amplitude doubles from 20 Hz to 30 Hz. The shear strains reach values for which pore pressure build-up can be expected [9], particularly for a large number of cycles and if the soil cannot dissipate the pore pressure. Such built-up pore pressure may also spread to critical parts of the slope through permeable layers which often exist in quick clay deposits of this kind. ([36]).

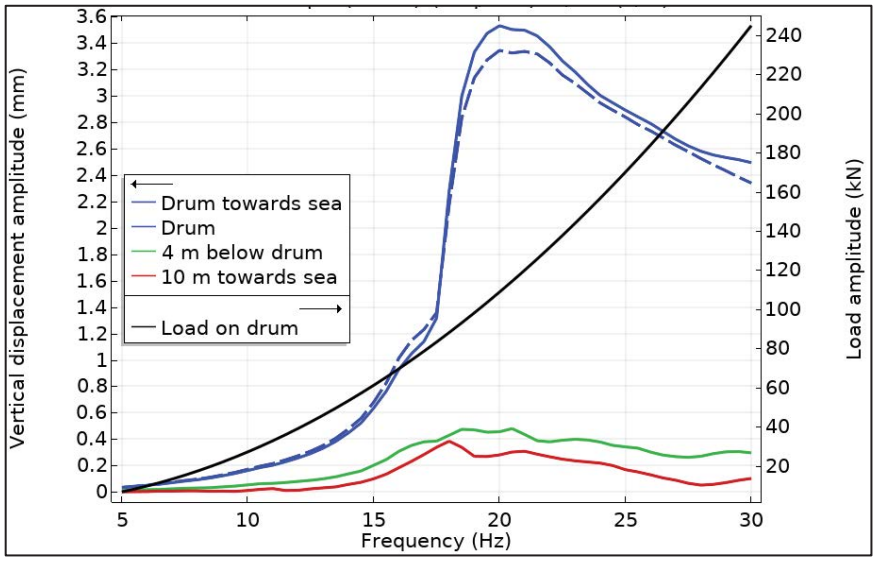

Figure 9 Vertical displacement amplitude (left axis) and load amplitude (right axis) versus loading frequency. Peak drum response at 20 Hz.

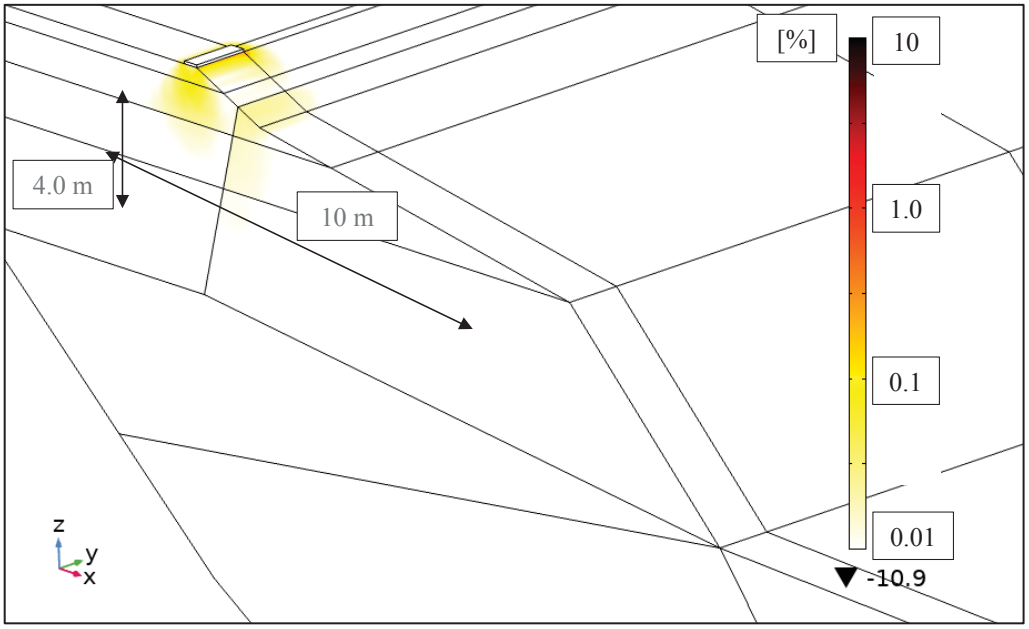

Figure 10 Maximum shear strain at 14 Hz for load amplitude of 53 kN. Colour scale is logarithmic from 0.01 % to 10% shear strain.

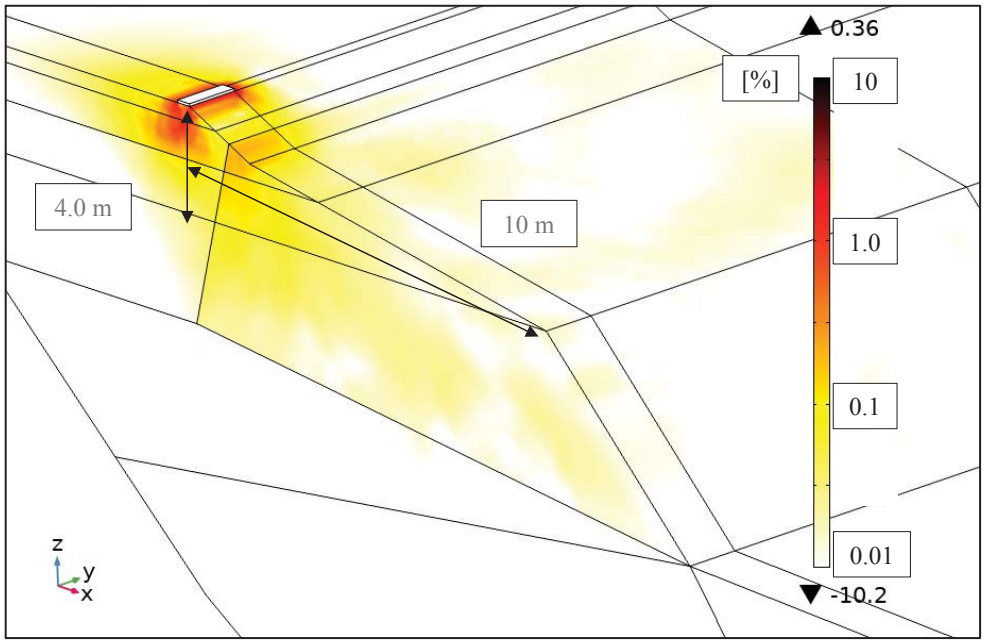

Figure 11 Maximum shear strain at 20 Hz. Colour scale is logarithmic from 0.01 % to 10% shear strain. At 10 m from the drum towards the slope the maximum shear strain reaches 0.025 %.

Using 2nd order elements allows improved capturing of large strain amplitudes around the vibrating plate (drum), and also reduces possible volumetric locking due to high Poisson's values in the submerged part of the slope. Figure 12 shows the response for the same model as in Figure 9, except for the use of 2nd order elements. The peak response of the drum now occurs at 15 Hz compared to 20 Hz for the model with linear element. The vibration amplitude of the drum is approximately the same as for 1st order elements with some increase to the sides of the drum due to local nonlinearity (see solid and dashed blue lines). However, the applied load amplitude on the drum is much lower with 61 kN at 15 Hz, compared to 109 kN at 20 Hz, which indicates the response is to stiff with the 1st order elements.

Using the 2nd order mesh discretization give a softer numerical behavior of the soil, and the frequency at the peak response of the drum-fill now coincides with the slope's natural vibration frequency of about 15 Hz. The vibration amplitude 4 m beneath and 10 m in front of the drum increase rapidly with frequency as shown with green and red curves in Figure 12. 4 m beneath the drum the maximum velocity amplitude is about 35 mm/s and 10 m towards the slope it is 20 mm/s. These velocity amplitudes correspond to shear strains high enough to cause pore pressure build up [9]. The double resonance, i.e. the coincidence of resonance frequency of the drum and compacted fill with the slope's natural vibration frequency likely have contributed to the relatively large shear strains induced.

The difference in response of the slope below and above the resonance frequency is also clearly seen in the plots of shear strains for 13 Hz and 16 Hz as shown in Figure 13 and Figure 14. Figure 14 shows a node-antinode wave pattern with regions of high shear strains surrounding areas with low shear strains.

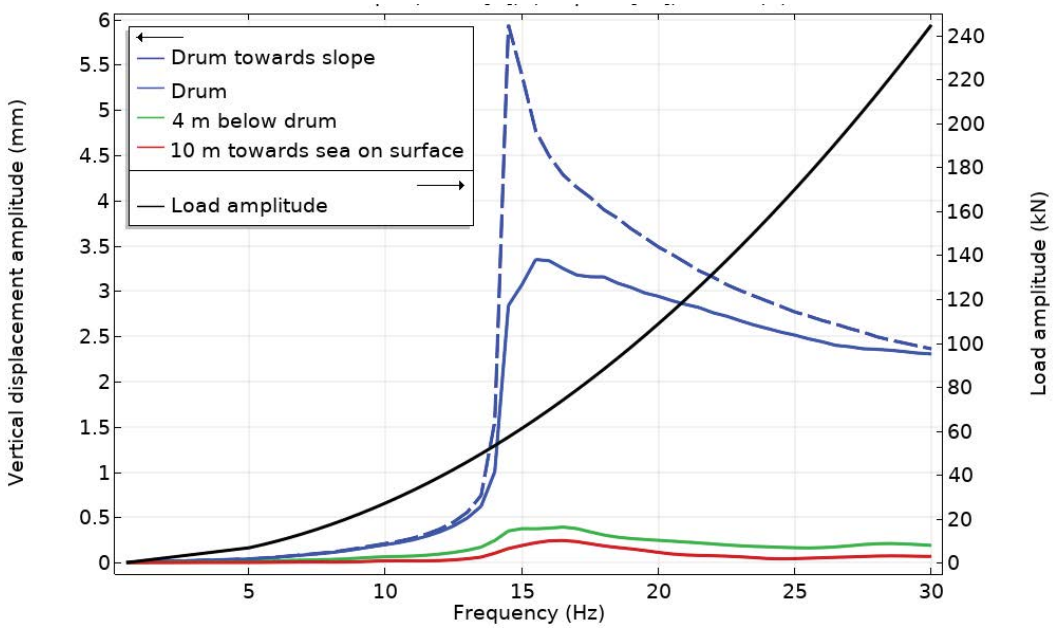

Figure 12 Vertical displacement amplitude (left axis) and load amplitude (right axis) versus loading frequency. Peak drum response at about 15 Hz.

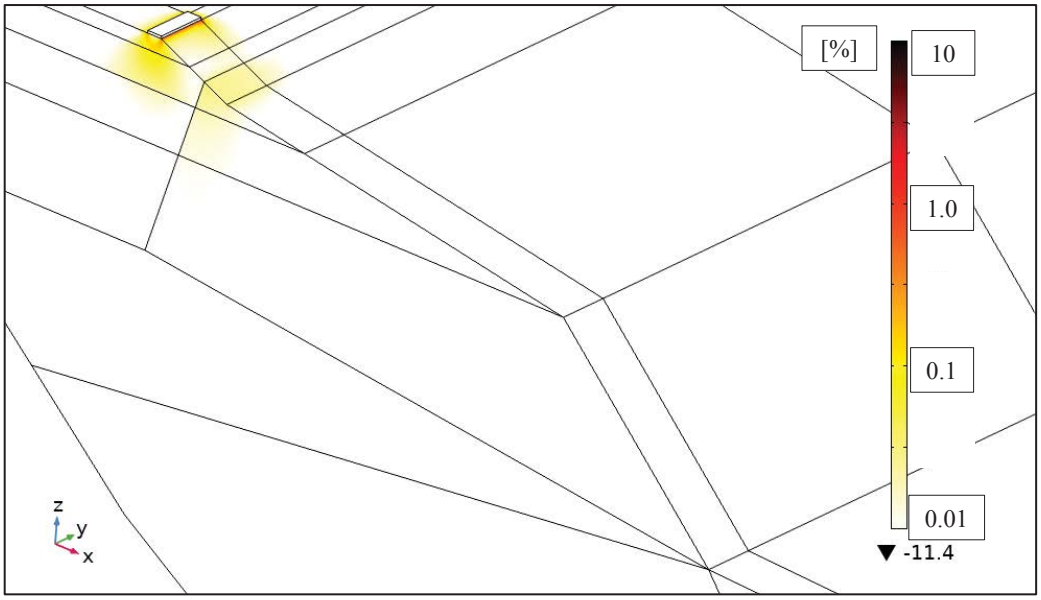

Figure 13 Maximum shear strain at 13 Hz for load amplitude of 46 kN. Colour scale is logarithmic from 0.01 % to 10% shear strain.

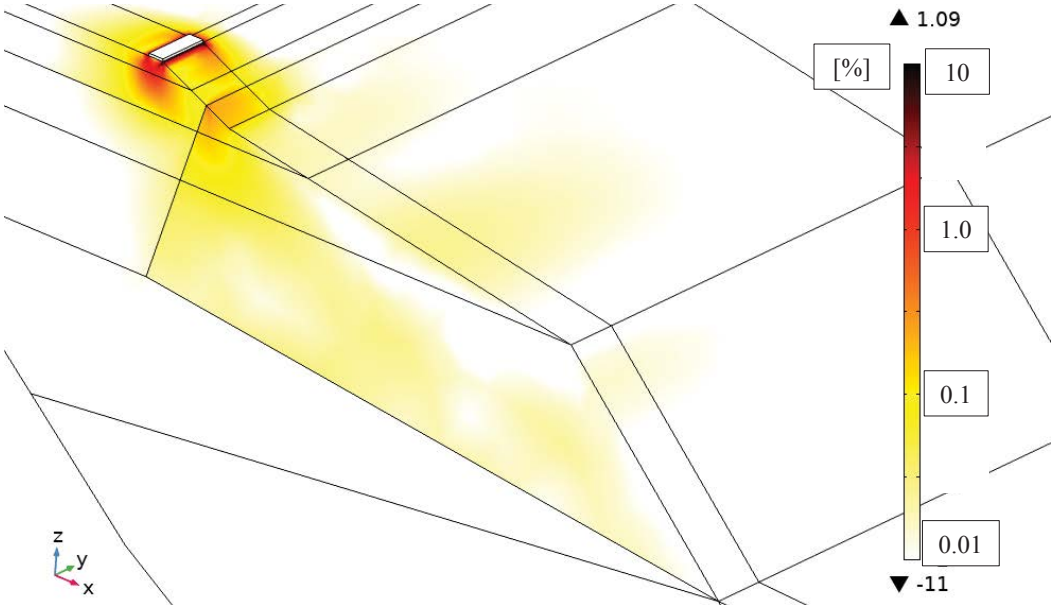

Figure 14 Maximum shear strain at 16 Hz. Colour scale is logarithmic from 0.01 % to 10% shear strain. At 10 m from the drum towards the slope the maximum shear strain reaches 0.025 %.

7.3 Effect of bouncing drum

To understand better the effect of a jumping drum on the slope stability and soil-nonlinearity we have compared the response for four different load amplitudes all at 15 Hz close to the natural frequency of the slope, at which vibrations can propagate out towards the slope surface. This comparison have so far only been done for 1st order elements, but give a qualitative indication.

Comparing static stress due to weight on the drum with dynamic stresses beneath it, indicates the drum may not be in contact with the soil in parts of the vibration cycle (i.e. it is bouncing). The non-contact situation starts at frequencies in the range 12-15 Hz in this analysis. The frequency range will vary with drum mass, load amplitude and the non-linear soil stiffness.

It is not fully correct to apply the equivalent linear method to the problem of a bouncing drum. However, the estimated vibration amplitudes are likely on the high side and thus it would be conservative to use the approach to estimate the effect of compaction on slope stability. As mentioned, the load acting on the drum is proportional to the square of the drum vibration frequency. Thus when the drum is bouncing, the load amplitude applied to the drum is controlled by the drum vibration frequency, even though the soil vibrates with a lower frequency.

The following analysis tries to capture the underlying mechanism causing the second vibration peak around 30 Hz as shown in Figure 6 a). A comparison of stiffness degradation at a vibration frequency of 15 Hz is given in Figure 15 a) - d) for load amplitudes of 67 kN (not bouncing), 101 kN (partial loss of contact), 134 kN (partial loss of contact) and 269 kN (double frequency bouncing at 30 Hz as shown in Figure 2 c) and in the experiment result Figure 6a). 269 kN is the load for a roller vibration frequency of 30 Hz.

For the lower load amplitude (67 kN) there is only stiffness degradation locally beneath the roller and some 30-40% reduction in the upper part of the old fill towards the sea. With increasing load amplitude, the stiffness reduction reaches deeper down, at 100 kN load the reduction is about 60% at a depth of 1.5 m. For a load of 134 kN the stiffness reduction is more than 60% down to 2-meter depth. For the large load amplitude of 269 kN the stiffness degradation is occurring in a larger soil volume down to some 4 meter depth and the old fill sustains larger stiffness degradation down to 2 meter depth.

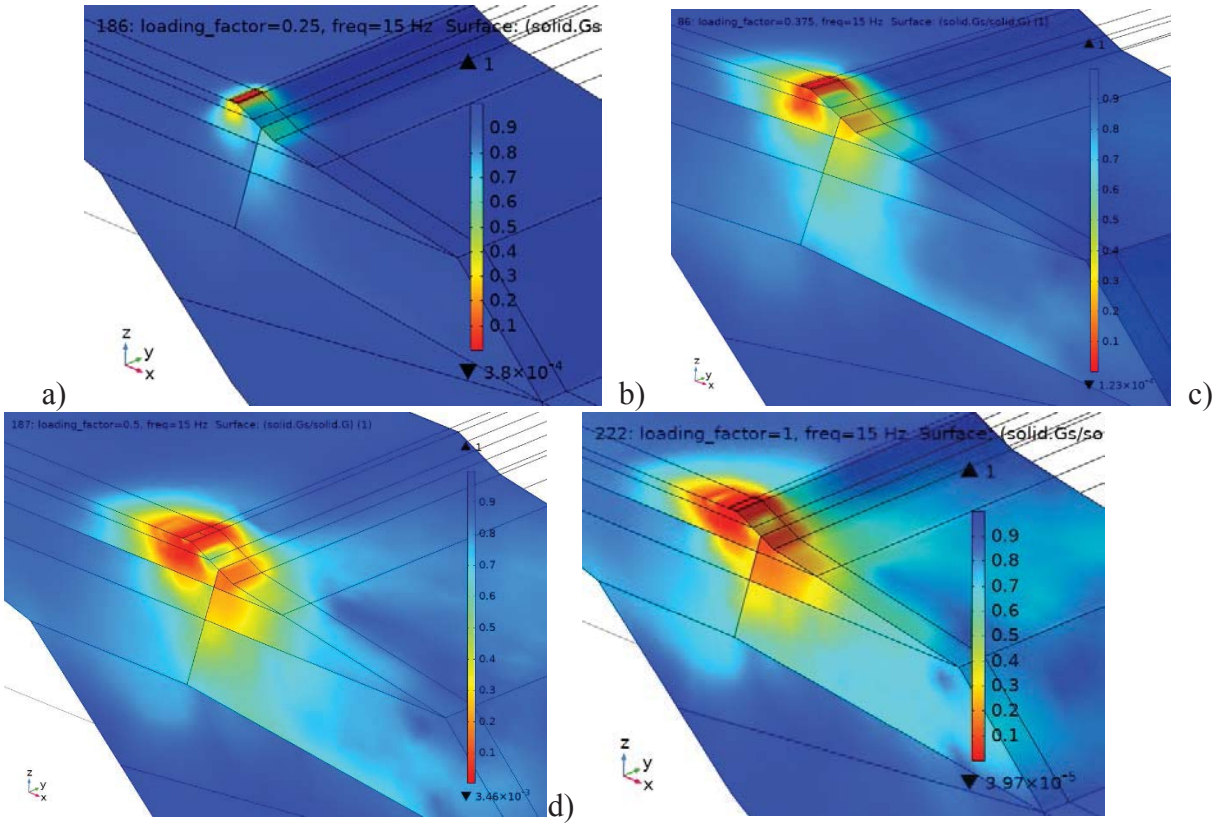

Figure 15 Reduction of shear modulus for a vibration frequency of 15 Hz for a load amplitude of 67 kN in a), corresponding to 25% of maximum load amplitude. In b) the load is 101 kN, in c) 134 kN and in d) the maximum load amplitude of 269 kN is applied.

8 DISCUSSION

There are usually many contributing factors when construction activities cause landslides. These could e.g. be unknown soil conditions, such as the presence of weak soil layers and artesian water pressures resulting in lower actual factors of safety than anticipated by the geotechnical engineer's stability analysis. In the case of vibratory compaction, one should consider the effect of increased weight from the fill, compaction induced increase in lateral pressures, and use of less heavy equipment [37]-[40].

Here we have to tried to understand how vibrations induced by compaction may affect the slope stability. The computed shear strains due to vibrations from compaction for the Statland case are large enough to cause pore pressure build up in the soft soil sediments [9]. Considering the very loose soil conditions as indicated by the post-slide investigation [1] it seems very likely the construction work caused the landslide and probably the vibratory compaction have contributed to the triggering. This confirms the conclusions in [1].

Vibrations were not measured for Statland case. Therefore it is not known how large the vibration amplitude was or how large the dynamic impact on the slope was. The analysis presented in this paper have tried to capture a range of possible load amplitudes and frequencies, to understand the effect of compaction on slope stability and if it is possible to establish a vibration limit to avoid slope failure. For practical reasons such limit values should be related to vibration measured on the ground surface. The vibration amplitude on the ground surface is very high near the vibratory roller, but attenuates quickly with distance. Since the roller is moving around when it operates it may be difficult to establish a vibration limit since the distance

to the roller is not known / varying all the time. Thus, the vibrations could be larger than measured by the vibration sensor. However, if one can measure vibrations on the ground surface at critical locations, e.g. on based slope stability analysis and tentatively keeping them lower than 20 mm/s it seems unlikely the vibrations could have negative effect on slope stability. In general, depending on the ground conditions and computed factor of safety for the slope stability, a slope can tolerate much larger vibration amplitudes than 20 mm/s.

The numerical analysis further indicate for a bouncing roller, i.e. the roller drum is fully in the air during every other soil vibration cycle, the effect on stiffness and strength degradation in the ground can be even larger. Thus avoiding bouncing of the drum is imperative when compacting in the vicinity of vibration sensitive soils. Many modern vibratory compaction rollers can sense and automatically reduce the jumping [15], [19].

The vibration frequency range of many vibratory rollers lies within a range such that when it bounces the frequency of impact on the ground may coincide with global natural vibration frequency of slopes. The performed numerical analysis indicates the global natural frequency of the slope is mainly controlled by the elastic shear wave speeds and geometry. The local soil-nonlinearity around the drum do not affect the global natural frequency. Further analysis is needed to understand the interplay ("double resonance") between the global natural frequency, the local natural frequency of the drum-soil, and how they are affected by soil nonlinear stiffness and slope geometry.

For load amplitudes large enough to cause jumping of the drum, the performed frequency domain analysis does not capture the partial or no-contact between the drum and the soil. Therefore the computed vibration amplitudes are likely on the high side. Further comparison with field measurements and non-linear time domain analysis are needed.

9 CONCLUSIONS AND RECOMMENDATIONS

The numerical analysis indicate vibratory compaction have possibly contributed to triggering the slide at Statland. The nonlinear analysis is believed to have captured the essential behaviour of the vibratory compaction and the response of the slope. The peak response at the frequency is close to the one stated by the operator of the vibratory roller and the manufacturer's data sheet.

To reduce the landslide risk during compaction work in the vicinity of slopes with vibration susceptible soils and low static stability near the shoreline the following is suggested

- Use less heavy equipment and/or higher loading frequencies or perform compaction without vibration. Avoiding excessive bouncing of the vibratory roller drum is imperative.
- Applying thinner layers and more time between compaction passes. Allowing for more time between placing of layers reduces the number of load cycles applied by the soil and allows for drainage of potential built up pore pressures both due to cyclic loading and due to static loading from weight of the fill.
- Monitor slope horizontal and vertical displacements at some critical points.
- Monitor pore pressures at critical points. Locations with artesian pressure have lower stability, any extra pore pressure from the compaction will reduce the stability of the slope.

10 ACKNOWLEDGEMENT

The financial support by the governmental research program "Natural Hazards: Infrastructure for floods and slides (NIFS)" and by the Norwegian Research Council through Remedy

project BegrensSkade II – Risk Reduction of Groundwork Damage Grant No. 267674, is gratefully acknowledged. The equivalent linear dynamic 3D tool sprung out of the collaboration with Prof. Staffan Hintze (NCC), Kenneth Viking (Swedish Transport Administration), and Fanny Deckner (GeoMind) financially supported by NCC and by the Development Fund of the Swedish Construction Industry, which is also highly appreciated.

REFERENCES

[1]NVE The landslide at Nord-Statland. Investigation of technical causes. Report nr. 93-2014. ISBN-nr. 978-82-410-1042-2, http://www.naturfare.no/_attachment/751994/binary/1007572, in Norwegian.

[2]NVE, "Dynamic loading and landslide hazard ", (in Norwegian, title: Dynamiske påkjenninger og skredfare) https://brage.bibsys.no/xmlui/handle/11250/2498527, Report nr. 16-2016, 2016.

[3]Johansson J., Bouchard S. L'Heureux JS. (2017) Vibratory Roller Influence Zone Near Slopes with Vibration Susceptible Soils. In: Thakur V., L'Heureux JS., Locat A. (eds) Landslides inl Sensitive Clays. Advances in Natural and Technological Hazards Research, vol 46. Springer, Cham.

[4]Johansson, J. and L 'Heureux , J.-S. Influence of vibratory compaction on slope stability — an ongoing research topic in Norway, Anniversary Symposium — 40 Years of Roller Integrated Continuous Compaction Control (CCC), D. Adam & S. Larsson (eds.), November 29th, 2018, Vienna, Austria

[5]Johansson, J. and Kaynia, A. M., Equivalent linear pseudostatic and dynamic modelling of vertically vibrating monopile, Marine Structures, accepted manuscript under revision, 2020

[6]Bernander, Stig, Progressive landslides in long natural slopes: Formation, potential extension and configuration of finished slides in strain-softening soils. 2011. 240 p. Doctoral thesis, Luleå University of Technology.

[7]Ekström, A., & Olofsson, T. (1985). Water and frost-stability risks for embankments of fine-grained soils. In From Proceedings of the Symposium on Failures in Earthworks, organized by the Institution of Civil Engineers, held in London, March 6-7, 1985.

[8]Hryciw, R., Vitton, S., and Thomann, T. (1990). ”Liquefaction and Flow Failure During Seismic Exploration.” J. Geotech. Engrg., 116(12), 1881–1899.

[9]Dobry, R., Vasquez-Herrera, A., Mohamad, R., and Vucetic, M. (1985). "Liquefaction flow failure of silty sand by torsional cyclic tests." Proc, Session on Advances in the Art of Testing Soils Under Cyclic Conditions, ASCE, 29-50.

[10]Vucetic, M. (1994). Cyclic Threshold Shear Strains in Soils. Journal of Geotechnical Engineering, 120 (12), 2208–2228. https://doi.org/10.1061/(asce)0733-9410(1994)120:12(2208)

[11]Cornforth, Derek, Landslides in Practice: Investigation, Analysis, and Remedial/Preventative Options in Soils, ISBN: 978-0-471-67816-8 April 2005 624 Pages,

[12] S. Bouchard, J.-S. L’Heureux J. Johansson S. Leroueil and D. LeBoeuf, "Blasting induced landslides in sensitive clays", Landslides and Engineered Slopes. Experience, Theory and Practice – Aversa et al. (Eds), 2016 Associazione Geotecnica Italiana, Rome, Italy, ISBN 978-1-138-02988-0.

[13] Johansson J., Løvholt F., Andersen K.H., Madshus C. and Aabøe R. "Impact of blast vibrations on the release of quick clay slides". ICSMGE 2013, Paris

[14] Glimsdal, S., et al. The 29th January 2014 submarine landslide at Statland, Norway—landslide dynamics, tsunami generation, and run-up. Landslides , 13 (6), 1435–1444. https://doi.org/10.1007/s10346-016-0758-7, 2016

[15] Adam, D., Pistrol, J.: "Dynamic roller compaction for earthworks and roller-integrated continuous compaction control: State of the art overview and recent developments"; Talk: Conferenze di Geotecnica di Torino, XXIV Ciclio, Turin (invited); 02-25-2016 - 02-26-2016; in: "Conferenze di Geotecnica di Torino, XXIV Ciclio", M. Manassero, A. Dominijanni, S. Foti, G. Musso (ed.); (2016), 1 - 41

[16] van Susante, P. J., & Mooney, M. A. (2008). Capturing Nonlinear Vibratory Roller Compactor Behavior through Lumped Parameter Modeling. *Journal of Engineering Mechanics*, *134*(8), 684–693. https://doi.org/10.1061/(asce)0733-9399(2008)134:8(684)

[17] Wersäll, C., Nordfelt, I., & Larsson, S. (2017). Soil compaction by vibratory roller with variable frequency. Géotechnique , 67 (3), 272–278. https://doi.org/10.1680/jgeot.16.p.051

[18] Wersäll, C., Nordfelt, I., & Larsson, S.. Resonant roller compaction of gravel in full-scale tests, Transportation Geotechnics, 14, 93–97, 2018, https://doi.org/10.1016/j.trgeo.2017.11.004

[19] Anderegg, Roland and Kuno Kaufmann Intelligent Compaction with Vibratory Rollers Feedback Control Systems in Automatic Compaction and Compaction Control. Transportation Research Record: Journal of the Transportation Research Board, No. 1868, TRB, National Research Council, Washington, D.C., 2004, pp. 124–134.

[20] Transportation Research Board, Intelligent Soil Compaction Systems, NCHRP report 676, 2010, http://www.trb.org/Publications/Blurbs/164279.aspx.

[21] Lysmer, J., Udaka, T., Tsai, C.F., Seed, H.B., 1975. FLUSH: A computer program for approximate 3-D analysis of soil-structure interaction problems, Report EERC 75-30, Earthquake Engineering Research Center, U.C.Berkeley.

[22] Schnabel, P.B., Lysmer, J., Seed, H.B., 1972. SHAKE: a computer program for earthquake response analysis of horizontally layered sites, Report EERC 72-12, Earthquake Engineering Research Center, U.C.Berkeley.

[23] Darendeli M. B., Development of a new family of normalized modulus reduction and material damping curves, Ph.D. Dissertation, The University of Texas at Austin, August, 2001.

[24] Groholski, D. R.; Hashash, Y. M. A.; Kim, B.; Musgrove, M.; Harmon, J. & Stewart, J. P., Simplified Model for Small-Strain Nonlinearity and Strength in 1D Seismic Site Response Analysis, Journal of Geotechnical and Geoenvironmental Engineering, American Society of Civil Engineers (ASCE), 2016, 142, 04016042

[25] Amir-Faryar, B.; Aggour, M. S. & McCuen, R. H., Universal model forms for predicting the shear modulus and material damping of soils, Geomechanics and Geoengineering, Informa UK Limited, 2016, 12, 60-71

[26] Wichtmann, T. & Triantafyllidis, T. Effect of Uniformity Coefficient on G/Gmax and Damping Ratio of Uniform to Well-Graded Quartz Sands Journal of Geotechnical and

Geoenvironmental Engineering, American Society of Civil Engineers (ASCE), 2013, 139, 59-72

[27]Andersen, K. H., Cyclic soil parameters for offshore foundation design, The Third ISSMGE McClelland Lecture, ISFOG III, Meyer, V. (Ed.), CRC Press, 2015

[28]Blaker, Ø., & Andersen, K. (2015). Shear strength of dense to very dense Dogger Bank sand. In Frontiers in Offshore Geotechnics III (pp. 1167–1172). CRC Press. https://doi.org/10.1201/b18442-175

[29]Løvholt, F., C. Madshus, and K. H. Andersen. "Intrinsic Soil Damping from Cyclic Laboratory Tests with Average Strain Development." Geotechnical Testing Journal 43 (forthcoming). https://doi.org/10.1520/GTJ20170411.[27][27]

[30] Park, J., & Kaynia, A. M. (2017). FE simulation of steady state wave motion in solids combined with a PML approach. Procedia Engineering, 199, 1556–1561. https://doi.org/10.1016/j.proeng.2017.09.054

[31] Robertson, P. K. (2009). Interpretation of cone penetration tests — a unified approach. Canadian Geotechnical Journal, 46 (11), 1337–1355. https://doi.org/10.1139/t09-065

[32] Kaynia, A.M., Kausel, E., and Madshus, C.M. (1998). “Impedances of Underwater Rigid Square Foundations.” Proc. ASCE Spec. Conf. Geotech. Earthquake Engng, Seattle, WA, USA, 1283-1293.

[33] J. Park and A.M. Kaynia, Stiffness matrices for fluid and anisotropic soil layers with applications in soil dynamics, Soil Dynamics and Earthquake Engineering, 115, 169-182, 2018.

[34] Volvo Construction Equipment. Specifications for SD 115 vibrocompactor.

[35] R.V. Rinehart and M.A. Mooney, "Measurement depth of vibratory roller-measured soil stiffness", Géotechnique, Volume 59, Issue 7, 01 September 2009, pages 609 –619.

[36] Hintze et. al., , Report 95. Effect on surrounding during pile and sheet pile installation (Omgivningspåverkan vid pål- och spontslagning), Swedish Pile commission, 1997 (in Swedish). http://www.palkommissionen.org/web/page.aspx?refid=86.

[37] Massarsch, K. R., 2002. ”Effects of Vibratory Compaction”. TransVib 2002 –International Conference on Vibratory Pile Driving and Deep Soil Compaction. Louvain-la-Neuve. Keynote Lecture, pp. 33 – 42.

[38] Chen, T.-J., & Fang, Y.-S. (2008). Earth Pressure due to Vibratory Compaction. Journal of Geotechnical and Geoenvironmental Engineering, 134(4), 437–444. https://doi.org/10.1061/(asce)1090-0241(2008)134:4(437)

[39] Canadian Geotechnical Society, "The Canadian Foundation Engineering Manual", 4th Edition, 2006.

[40] Norwegian Public Roads Administration, (NPRA), Handbook in road construction, N200 (in Norwegian), July 2018.